Virology **267,** 289–298 (2000)
doi:10.1006/viro.1999.0134, available online at http://www.idealibrary.com on IDEAL®

Membrane Interaction of Influenza Virus M1 Protein

Rob W. H. Ruigrok,*[1] Annie Barge,* Peter Durrer,† Josef Brunner,† Kai Ma,‡ and Gary R. Whittaker‡

*EMBL Grenoble Outstation, BP 156, 38042 Grenoble Cedex 9, France; †ETHZ, Biochemie, Universitätstrasse 16, CH-8092 ETH Zentrum, Zürich, Switzerland; and ‡Veterinary Medical Center, Cornell University, Ithaca, New York 14853

Received September 17, 1999; returned to author for revision December 2, 1999; accepted December 13 1999

The M1 protein of influenza virus is thought to make contact with the cytoplasmic tails of the glycoprotein spikes, lipid molecules in the viral membrane, and the internal ribonucleoprotein particles. Here we show electron micrographs of negatively stained virus particles in which M1 is visualized as a 60-Å-long rod that touches the membrane but apparently is not membrane inserted. Photolabeling with a membrane restricted reagent resulted in labeling of the transmembrane region of haemagglutinin but not of M1, also suggesting that most of M1 is not embedded into the hydrophobic core of the viral membrane. Finally, *in vitro* reconstitution experiments using soluble M1 protein and synthetic liposomes or Madin–Darby canine kidney cell membranes suggest that M1 can bind to negatively charged liposomes and to the cellular membranes and that this binding can be prevented under high-salt conditions. Although none of these experiments prove that there does not exist a minor fraction of M1 that is membrane inserted, it appears that most of M1 in the virus is membrane associated through electrostatic interactions.

Key Words: influenza virus; matrix protein; electron microscopy; hydrophobic photolabeling; M1 membrane floatation.

INTRODUCTION

Influenza virus is a negative-strand RNA virus with eight ribonucleoprotein particles (RNPs) contained within a lipid envelope. Two glycoproteins, haemagglutinin and neuraminidase, extend outward from the lipid membrane, and a third intramembrane protein, M2, forms a tetrameric membrane channel (Lamb and Krug, 1996). Inside, lining the membrane, is a layer of M1 protein (27 kDa). Influenza virus does not appear to be built with icosahedral symmetry and is notoriously variable in size and shape. Estimates of the copy number of M1 per virus particle are also variable, ranging from 1100 to 3000 (Ruigrok *et al.,* 1989; Lamb, 1989; Lamb and Krug, 1996), probably depending on the level of purity and polydispersity of the virus suspension that was used to determine this value. M1 is essential for budding and is thought to be involved in contacts with the RNPs and the membrane (Oxford and Hockley, 1987). Recently, it was shown that the cytoplasmic tails of the glycoproteins are needed for correct virus assembly (Mitnaul *et al.,* 1996; Jin *et al.,* 1997), and it is assumed that M1 interacts with these tails on the inside of the viral membrane.

Electron micrographs of thin sections and cryoelectron micrographs of vitrified samples show additional material adhering to the inner surface of the membrane, which was interpreted as the M1 protein layer (Nermut, 1972; Schulze, 1972; Booy *et al.,* 1985; Fujiyoshi *et al.,* 1994). Schulze (1972) estimated that this protein layer was about 60 Å thick. When influenza virus is prepared for electron microscopy (EM) by negative staining with sodium silicotungstate (SST) or phosphotungstic acid (PTA) and when the viral membrane is damaged during this procedure, the stain may enter the virus particle, leading to visualization of the M1 protein layer. The M1 monomers can be seen as highly contrasted dots (end-on view) making up rows (see Fig. 1 and Nermut, 1972; Schulze, 1972; Wrigley, 1979; Ruigrok *et al.,* 1989). The dots are spaced about 40 Å along the rows, and the rows are also about 40 Å apart (1 Å = 0.1 nm) (Ruigrok *et al.,* 1989).

It has been generally accepted that M1 is inserted into the viral lipid bilayer (Bucher *et al.,* 1980; Gregoriades, 1980; Gregoriades and Frangione, 1981). Recently, the atomic structure of the N-terminal two thirds of influenza virus A/PR/8/34 M1 protein was solved (Sha and Luo, 1997). The molecule is hydrophilic on the outside, and the noncharged residues thought to be involved in membrane embedding are at the inside of the molecule. The authors of the M1 structure paper have therefore suggested that the M1 molecule has to fold inside-out for membrane insertion.

Here we studied M1 membrane interaction by EM on intact virus, on detergent-solubilised spikeless virus, and on purified M1 protein. We also performed hydrophobic photolabeling experiments on M1 in virus and studied the *in vitro* interaction of M1 with membranes. Although none of our results can exclude the possibility that a minor fraction of M1 is membrane inserted, the data

[1] To whom reprint requests should be addressed at EMBL Grenoble Outstation, c/o ILL, 6 Rue Jules Horowitz, 38000 Grenoble, France. Fax: +33-4-76-20-71-99. E-mail: ruigrok@embl-grenoble.fr.

0042-6822/00 $35.00

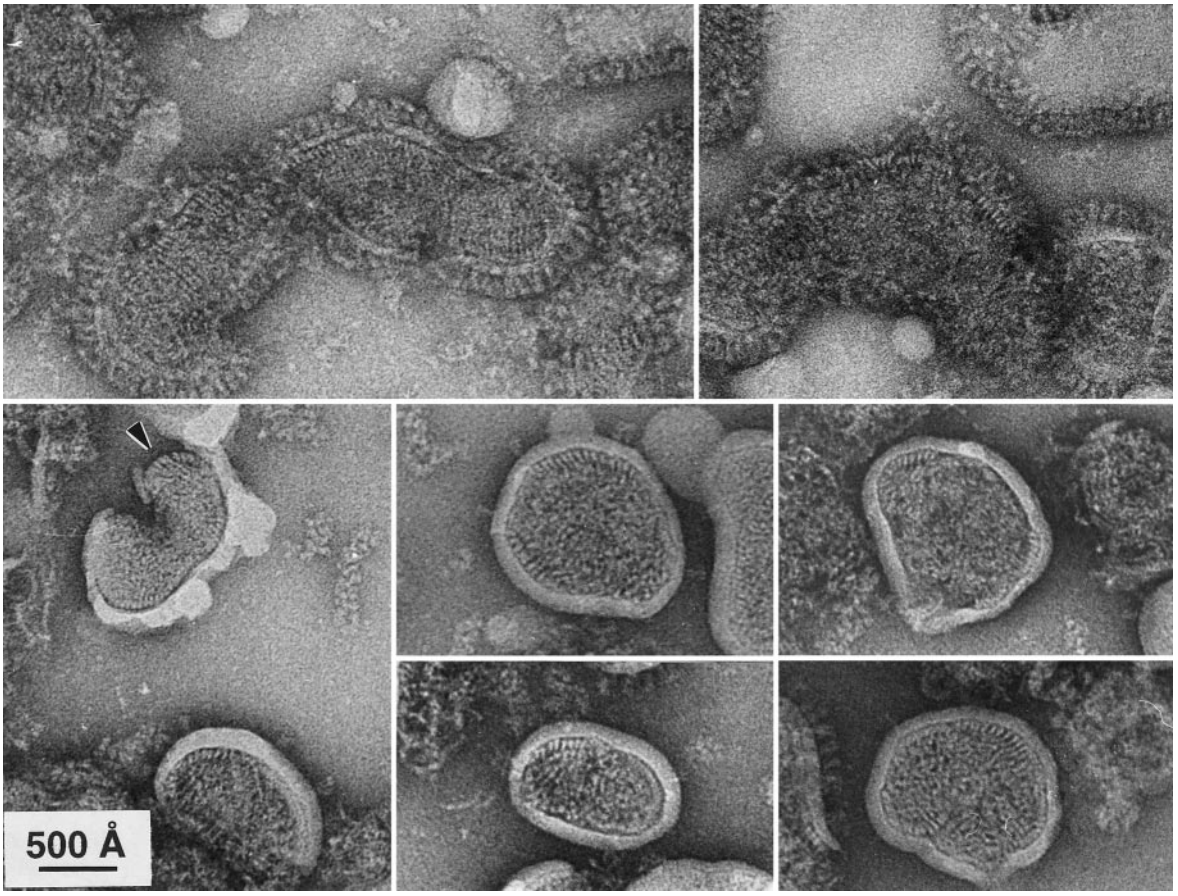

FIG. 1. Electron micrographs of negatively stained influenza A/PR/8/34 virus. (Top) Intact virus. (Bottom) Spikeless virus after bromelain treatment (Brand and Skehel, 1972). The stain (SST) has penetrated the virus particles and outlines the submembranal layer of M1 protein. At the membrane, M1 can be seen in side view as 60-Å-long, white rods. The arrowhead indicates a region where the lipid bilayer has separated from the core structure, probably during preparation for EM, where the 60-Å rods are still visible. The bar represents 500 Å.

suggest that the major proportion of M1 in virus is associated with the membrane through electrostatic interactions.

RESULTS

EM of influenza virus M1

To examine the nature of the interaction of M1 with the membrane, we first carried out electron microscopic examination of influenza A/PR/8/34 virus particles stained with SST or PTA. The images showed the previously reported rows of dots below the membrane shell as mentioned in the introduction. In cases in which the M1 was visualized in contact with the membrane, radially arranged rods were seen rather than the dots described previously (Fig. 1). Pictures with such rods can be seen in previously published micrographs of negatively stained virus (see, for example, Fig. 10 in Nermut, 1972), but their significance has up to now been ignored. The rods were seen with intact virus (Fig. 1, top) and with bromelain-treated spikeless virus (Fig. 1, bottom six particles) that contains no structures other than the RNPs, the M1 layer, and the lipid membrane (Brand and Skehel, 1972). In intact virus, the rods have a length of 59 $\pm$ 4 Å (25 measurements), and in spikeless virus, we measured virtually the same length of 58 $\pm$ 4 Å (40 measurements). The rods are seen to be regularly arranged, approximately perpendicular to the circular projection of the lipid membrane. We interpret the rods as a side view of the M1 monomer, and the dots in the rows as an end-on view. This means that M1 is a thin rod of about 60 Å in length, touching the membrane with one of its thin ends. The rods make up a lattice perpendicular to the membrane with spacing of about 40 $\times$ 40 Å (but this does not mean that the rods are 40 Å in diameter). Note that the 60-Å length corresponds with the width of the M1 layer determined previously by Schulze (1972). The micrographs further show that the stain-filled separation between the rods and the membrane is variable in width and that the membrane can even peel away after bromelain treatment and staining for EM, leaving the rods of M1 protein behind (Fig. 1A, arrowhead). This suggests that the M1 rods that are visualized here are membrane associated rather than membrane inserted.

The shape of detergent-solubilised M1 was also studied. Spikeless A/PR/8/34 virus was disrupted with Triton X-100 and centrifuged over a glycerol gradient. The gradient fractions were analyzed on an SDS–polyacrylamide gel (Fig. 2A). Solubilised, monomeric M1 protein remained at the top of the gradient (Fig. 2A, lanes B). These two fractions, which contain only M1 protein, were combined and dialyzed against PBS and prepared for EM by negative staining with SST. Most of the particles in the EM preparation were visible as small dots, probably representing individual M1 protein monomers, but were too small and irregular to provide reliable information on the shape of the molecules (not shown). However, some of the M1 protein had polymerized into flexible ribbons (Fig. 2B). This polymerization must have happened during the dialysis step because otherwise these polymers would have sedimented further into the gradient. Local order in these ribbons was sometimes observed over short distances (indicated by arrowheads in Fig. 2B), suggesting that the ribbons are made up by side-to-side association of thin rods with a length of 57 ± 5 Å (43 measurements), which defines the width of the ribbon. The monomers are spaced at 35 ± 5 Å (44 measurements) intervals, similar to the spacing of M1 in virus. Lower in the glycerol gradient, M1 cosedimented with RNP (Fig. 2A, lanes C). This sample was also examined by microscopy after removal of the glycerol by dialysis. Here, among the RNP complexes, we observed another polymer of M1, consisting of a small coil (Fig. 2C, top panel for side views and bottom panel for end-on views of the coils). The stain distribution in the rightmost structure in the lower panel of Fig. 2C suggests that this M1 polymer is a coil rather than a stack of rings. In both views, it can be seen that the coils are made up by subunits with a spacing of 35–40 Å and the turns of the coils are spaced at 44 Å. These dimensions are also similar to the spacing of the M1 monomers in the intact virus (Ruigrok *et al.,* 1989). In the end-on view, it can be seen that the turns of the coils are made up by rods that are slightly skewed with respect to the ring axis and are 60 ± 3 Å (17 measurements) long.

Figure 2D shows isolated and purified influenza virus nucleoprotein (NP) that also forms polymeric rings on self-association (Ruigrok and Baudin, 1995). Although the NP monomers have a similar length as the M1 monomers [62 Å for NP (Ruigrok and Baudin, 1995) versus 57–60 Å for M1 (current study)], the monomers in the NP rings are clearly fatter, more triangular, and organized differently than the M1 monomers in the M1 coils in Fig. 2C. As a result of this, for similar size rings, there are 11–13 NP monomers versus 21–23 M1 monomers per ring. Furthermore, when NP polymerizes into larger structures, these look identical to viral RNPs (Fig. 2D, bottom), but NP does not form coils like those shown in Fig. 2C. On the bases of these morphological differences, we suggest that the coils in Fig. 2C consist of M1 protein and that the combined results from Figs. 2B and 2C suggest that isolated M1 can form polymers made up from thin rods that are 57–60 Å long. Because this is the same as the length of the thin rods inside virus particles, this also suggests that the M1 rods as visualized in Fig. 1 are not inserted into the lipid membrane to any significant length.

Photolabeling of M1 inside virus

To further address the question of membrane insertion of M1, we performed photolabeling experiments with [^{125}I]iodo-4-(trifluoromethyl-3*H*-diazirin-3-yl)benzyl benzoate (^{125}I-TID-BE) on intact influenza A/PR/8/34 virus as described by Durrer *et al.* (1995). This probe is very hydrophobic, and after irradiation with light, a very reactive and short-lived carbene group is formed that reacts even with saturated C—H bonds (for reviews, see Brunner, 1989, 1993). The virus was incubated with the probe, irradiated, and then analyzed on SDS–PAGE. Under reducing conditions (Figs. 3A and 3B, lanes 1), the label is exclusively associated with the HA_2 subunit of haemagglutinin, which contains the *trans*-membrane region. Under nonreducing conditions (Figs. 3A and 3B, lanes 2), the HA_1 and HA_2 subunits are not separated, and it is the intact haemagglutinin molecule that is labeled. A small amount of label in Fig. 3B (lane 2; 4% compared with the amount of label associated with intact HA) can still be seen at the level of HA_2, probably due to cleavage of a small fraction of HA due to running of the reducing and nonreducing samples on the same gel. However, M1 protein does not seem to be labeled with the probe. A similar experiment was performed on influenza A/X-31 virus with the same result: No labeling of M1. In fact, many labeling experiments have been performed on influenza virus with the aim of elucidating the conformational changes of haemagglutinin related to membrane fusion (for a review, see Gaudin *et al.* 1995). In all of these experiments, in which a variety of membrane-embedded probes were used, only labeling of HA was observed, never labeling of M1.

In Fig. 3B, the band for the M2 membrane-embedded protein was run off the gel, and we also did not see a band for NA. In the gel in Fig. 3A, we also did not see a band for NA at the level of the monomer (60 kDa). The egg-grown viruses that we used for this study seem to contain only a very small proportion of NA. From EM pictures on low pH and trypsin-treated virus, we could determine that there were fewer than 25 NA tetramers per virion (Ruigrok *et al.,* 1986, and unpublished results), which means less than 5% of total spikes. Because we see no labeled NA and because there are at least as many M1 monomers as NA plus HA monomers, this could mean that when 5% of M1 in the virus would be inserted into the hydrophobic interior of the membrane, we might not be able to detect it.

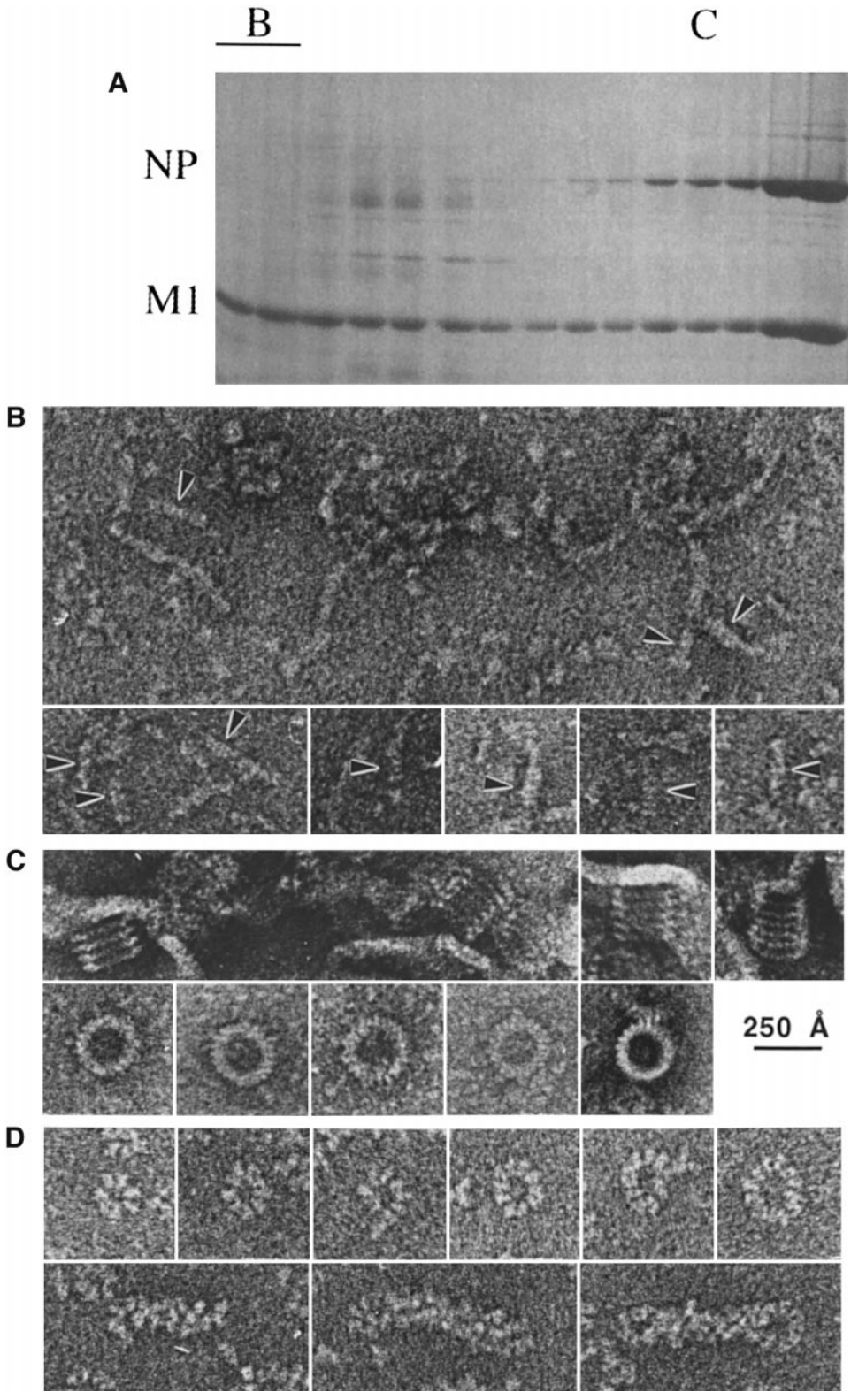

FIG. 2. Characterization of detergent-solubilised M1 protein. Spikeless A/PR/8/34 virus was disrupted with 1% Triton X-100 and centrifuged over a 10–30% glycerol gradient as described in Materials and Methods. The fractions were analyzed on SDS–PAGE (panel A; the top of the gradient is on the left). The top fractions, lanes B, were dialyzed against PBS and observed after negative staining. Micrographs of structures found in fraction B are shown in panel B of the figure. Arrowheads point out parts of the ribbons where a repeat of thin rods is visible. These rods are interpreted as a side-by-side arrangement of M1. Panel C shows micrographs of coils of M1 protein found in fraction C of the gradient. Fraction C also contained the easily recognizable RNP particles, but these are not shown in this figure. Panel D shows purified nucleoprotein free from M1 and free from RNA, as described by Ruigrok and Baudin (1995) (see text for details). All micrographs have the same magnification as indicated by the bar representing 250 Å.

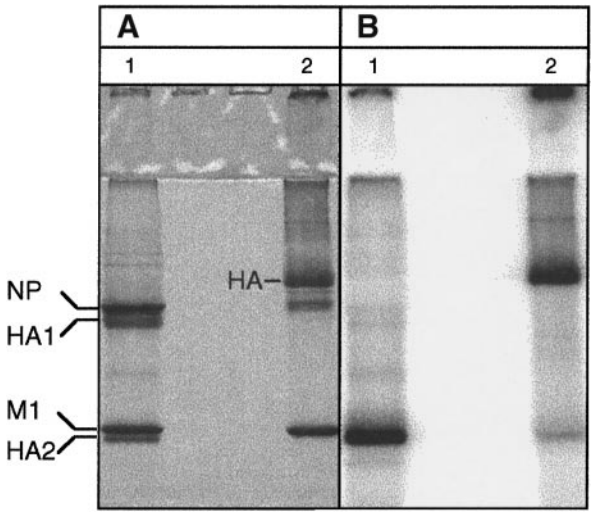

FIG. 3. Photograph-labeling experiment on intact influenza A/PR/8/34 virus. After photolabeling with ^{125}I-TID-BE, A/PR/8/34 viral proteins were dissolved in reducing (lane 1) or nonreducing (lane 2) sample buffer and subjected to 12% SDS–PAGE. The gel was stained with Coomassie Brilliant Blue R-250 (A) and subjected to autoradiography (PhosphorImager) (B). HA (1 and 2), haemagglutinin (subunits 1 and 2); M1, M1 protein.

In vitro association of M1 with liposomes and cellular membranes

We next tested the interaction of purified recombinant M1 protein with synthetic liposomes. We performed similar experiments as those that were described for the interaction of vesicular stomatitis virus (VSV) M protein with liposomes (Zakowski *et al.,* 1981), which showed that VSV M protein binds only to negatively charged liposomes and that this binding could be prevented by high salt. Figure 4A shows floatation experiments of purified recombinant M1 protein with liposomes of different compositions. It is clear that M1 binds only to liposomes containing at least 50% of the negatively charged phosphatidyl serine (PS). Liposomes that contained 75% PS also bound M1 protein, but because these liposomes are less stable, they did not float to the very top of the gradient. Then we tested the influence of the NaCl concentration of binding of M1 to liposomes containing 50% PS. From Fig. 4B, it is clear that binding was prevented at 500 mM NaCl and that at 400 mM, more than half of M1 did not bind. These experiments suggest that the interaction of soluble recombinant M1 with liposomes is electrostatic and that binding probably involves positively charged amino acids at the surface of M1. The binding characteristics of influenza virus M1 to liposomes are similar to those of the VSV M protein–liposome interaction (Zakowski *et al.,* 1981).

To analyze the binding of M1 to authentic cellular membranes, we performed binding assays using influenza M1 produced by an *in vitro* transcription/translation procedure and a preparation of total membranes from Madin–Darby canine kidney (MDCK) cells. M1 produced by *in vitro* transcription/translation was mostly soluble and remained soluble in a dilute solution in 50 mM phosphate buffer, pH 5.5. Binding assays were performed and M1 association with membranes was monitored by cosedimentation of M1 with membranes. In the absence of membranes, little M1 was visible in the pelleted material (Fig. 5A, lane 1). When cellular membranes were included in the assay, M1 cosedimented with the membranes (Fig. 5A, lane 2). To investigate the nature of the M1 cellular membrane interaction, we repeated the assay under conditions known to strip peripheral membrane proteins. We first included 1.5 M NaCl in the binding buffer. In this case, M1 no longer pelleted with the membranes (Fig. 5A, lane 3) and was present in the soluble fraction to levels essentially indistinguishable from the no-membrane control. We also incubated the M1 with membranes in high-pH carbonate buffer (0.1 M sodium carbonate, pH 11.5). In a similar manner to the high-salt treatment, M1 did not bind to membranes at

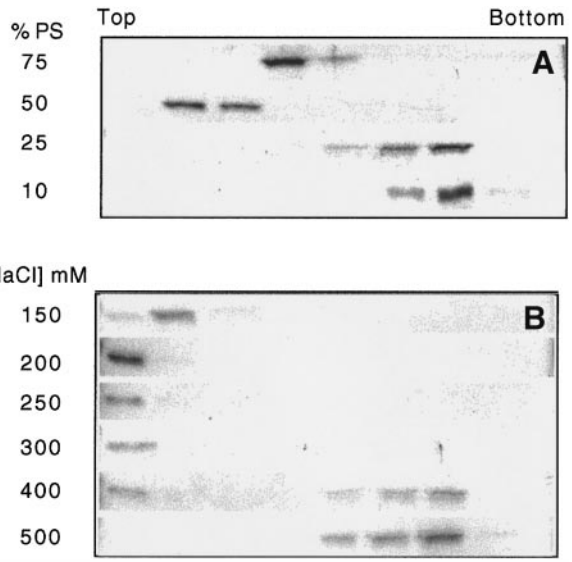

FIG. 4. Recombinant M1 liposome flotation experiments. Interaction of recombinant M1 with liposomes was tested in flotation experiments using various lipid compositions and various NaCl concentrations. The figure shows composite panels of two experiments. Each panel consists of parts of SDS–polyacrylamide gels stained with Coomassie G-250 showing only the region of the gels that contained the bands for M1 (there were no other bands on the gels). The rightmost lanes in the gels are the pellet fractions. (A) Dependence of M1 liposome interaction on lipid composition. M1 was mixed with lipids, buffer, and octyl glucoside, and after dialysis, the M1 liposomes were subjected to flotation centrifugation and the various gradient fractions were analyzed by SDS–PAGE. The lipid composition is given on the left of the gel, with 10% indicating 10% PS, 40% PC plus 50% cholesterol; 25% indicating 25% PS, 25% PC plus 50% cholesterol; 50% indicating 50% PS plus 50% cholesterol; and 75% indicating 75% PS plus 25% cholesterol. The salt concentration during the flotation experiment was 150 mM NaCl. (B) Dependence of M1 liposome interaction on salt concentration. M1 was added to preformed (50% PS plus 50% cholesterol) liposomes, and after incubation in buffer plus various NaCl concentrations, it was tested for lipid binding in a flotation experiment.

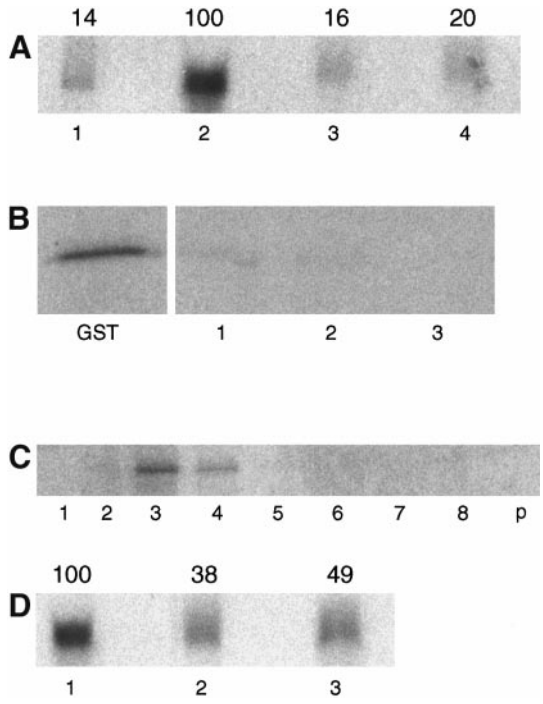

FIG. 5. Binding of *in vitro* transcribed/translated M1 to cellular membranes. A, C, and D are autoradiographs of ^{35}S-labeled *in vitro* transcribed/translated M1, and B shows *in vitro* transcribed GST. A, B, and D are pellet fractions, and C shows the fractions from an entire gradient. (A) Sedimentation of M1 with cellular membranes. Lane 1, M1 without membranes. Lane 2, M1 plus membranes in 50 mM phosphate buffer, pH 5.5. Lane 3, M1 plus membranes in 10 mM Tris • HCl, pH 7.4, 1.5 M NaCL, and 10 mM EDTA (high salt). Lane 4, M1 plus membranes in 0.1 M sodium carbonate buffer, pH 11.5 (high pH). The numbers above the lanes indicate the radioactivity in each lane compared with the 100% in lane 2. (B) GST-membrane binding control. GST was incubated with membranes and pelleted like M1 in panel A in pH 5.5 phosphate buffer (lane 1), high salt (lane 2), or high pH (lane 3). (C) Reflotation of pelleted M1 membrane complexes. M1 membrane complexes were pelleted as in panel A (lane 2), resuspended, and recentrifuged in a flotation assay. Lanes 1–8 are gradient fractions, and lane P is the pellet. Top of the gradient is at lane 1. (D) M1 release assay. M1 was pelleted with membranes as in lane 2 of panel A and resuspended in pH 5.5 phosphate buffer (lane 1), high-salt buffer (lane 2), or high-pH buffer (lane 3). The numbers above the lanes indicate the amount of radioactivity compared with the 100% in lane 1.

high pH (Fig. 5A, lane 4). As a control, we analyzed the membrane binding of glutathione-*S*-transferase (GST) in our sedimentation assay. No GST could be detected in the membrane pellet, either in the presence of absence of MDCK total membranes (Fig. 5B).

To confirm that the M1 in our sedimentation assay was not simply aggregating on contact with membranes, we resuspended the membrane bound M1 in buffer containing 80% sucrose and layered this under a 65–30% sucrose cushion. After centrifugation, the M1 membrane complex floated up to the 30% sucrose layer at the same position as total membranes without M1, as assessed by a Western blot using an anti-calnexin antibody (kindly provided by A. Helenius, ETH, Zürich). No M1 was found in the pellet fractions (Fig. 5C).

To investigate the stability of the M1 membrane interaction, we resuspended the membrane-bound M1 and repelleted the membranes. The M1 was again found in the pellet fraction, with little or no soluble material (Fig. 5D, lane 1). However, when we resuspended the pellet in the buffer containing high salt or at high pH as above, 60% or 50% of M1 protein, respectively, was released into the soluble fraction (Fig. 5D, lanes 2 and 3). These data confirm that stable association of M1 with membranes is mediated by electrostatic interactions. The fact that not 100% of M1 was resolubilized at high salt or high pH could be due to the fact that inside-out vesicles were formed during the first pelleting step, isolating M1 from the high-pH or -salt environment. On the other hand, it could also mean that a fraction of M1, once it has initially bound to the membrane by electrostatic interactions, proceeds to a tighter association that can no longer be disrupted by methods that would dissociate peripheral membrane proteins.

DISCUSSION

Here we present results from three very different experimental approaches that all point in the same direction: influenza virus M1 protein can bind to membranes through electrostatic interactions. This goes against the generally accepted idea that M1 protein is membrane inserted, which is mainly based on earlier work by Bucher *et al.* (1980), Gregoriades *et al.* (1980), and Gregoriades and Frangione (1981). In particular, our photolabeling experiments that suggest that most of M1 is not embedded into the hydrophobic core of the membrane differ from the earlier results reported by Gregoriades and Frangione (1981). The probe that was used in the present study is probably more hydrophobic and displays different photochemical behaviour than pyrene sulfonyl azide, the reagent used in the 1981 study. A less hydrophobic probe may not necessarily insert into the lipid bilayer yet interact with noncharged regions on the polypeptides. However, we must insist on the fact that although our experiments suggest that most of M1 is attached to the membrane in an electrostatic fashion, they do not exclude the possibility that a minor fraction of M1 is membrane inserted. The detection limit for membrane anchored proteins in the photolabeling assay may be 5–10%, and the M1 membrane reconstitution experiments did not give 100% definitive results, in particular for the M1 release experiment. Further, the EM pictures shown in Fig. 1 do not exclude the possibility that some M1 protein is not rod like but has another conformation and is membrane inserted. Any membrane-inserted M1 showing less regular details than the rods would probably have been overlooked.

Another problem with the micrographs shown in Figs. 1 and 2 is that the identification of M1 is only morphological. The structures made by what we interpret to be

M1 are different from those made by RNP or by purified NP. Positive identification of proteins in EM could, in principle, be done by immunogold labeling. However, M1 in the virus in Fig. 1 is still contained within the viral lipid envelope. To label M1, the lipid has to be removed by detergent treatment, leading to destabilization of the M1 arrays. Another aspect of immunolabeling is that nonspecific labeling needs to be prevented by using blocking proteins, just like in a Western blot. These blocking proteins will interfere with the outlining of the M1 arrays by the negative staining procedure. Although we have extensively tried to obtain immunolabeling of M1 arrays, we were never able to see the gold label and the fine details at the same time. Murti *et al.* (1992) also tried to label the internal structures of influenza virus. They concluded that labeling with antibodies against M1, NP, and the P proteins was possible only on degradation of the structures.

There have been a number of studies that have addressed M1 membrane association of protein expressed alone or with other viral proteins in a vaccinia T7 system (Kretzschmar *et al.,* 1996; Zhang and Lamb, 1996) or of M1 membrane association during an actual influenza viral infection (Enami and Enami, 1996; Zhang and Lamb, 1996). With transient expression of M1, Kretzschmar *et al.* (1996) found that 10–20% of M1 associated with membranes and that the protein could not be dissociated from the membranes by high salt or high pH. However, when these authors made mutants in the hydrophobic sequences of M1 that were supposed to be the membrane-inserted regions of the protein (Gregoriades and Frangione, 1981; Ye *et al.,* 1987), the mutant proteins associated with membranes to the same extent and with the same characteristics as wild-type M1. Zhang and Lamb (1996) found much more membrane association with transiently expressed M1 (45% at 0 time and 68% after a 3-h chase period). However, in their hands, the membrane-associated M1 protein behaved as neither an integral membrane nor a peripheral membrane-associated protein. When they performed a detergent partitioning experiment with Triton X-114, both the membrane-bound and the soluble M1 fractions partitioned about 50:50 in the detergent and water phases. It is also worth noting that Garoff and coworkers (Zhao *et al.,* 1998) found a significant fraction of SFV-expressed influenza virus M1 rapidly associated with cellular membranes, which was partially sensitive to high-salt and high-pH treatment. Whatever the nature of the M1 membrane interaction in these transfection experiments, it seems unlikely that it occurs through regular membrane insertion of the specific amino acid sequences identified by Gregoriades and Frangione (1981) and Ye *et al.* (1987).

The membrane association behaviour of M1 during an actual virus infection is even more complicated. Although large amounts of M1 are seen associated with membranes in a membrane flotation assay (Enami and Enami, 1996; Zhang and Lamb, 1996) much of M1 seems to be attached to the cytoskeleton (Zhang and Lamb, 1996; Avalos *et al.,* 1997), and it seems that at least part of the association of M1 with membranes may occur through membrane–cytoskeleton interaction (Zhang and Lamb, 1996). Interaction of M1 with the cytoskeleton does not occur when M1 is expressed out of the context of the influenza virus infection and may be mediated by other viral components (Zhang and Lamb, 1996; Avalos *et al.,* 1997).

The biochemical behaviour of M1 corresponds better to electrostatic membrane interaction than to hydrophobic interaction. M1 can be isolated by destabilization of the viral membrane with a detergent in the presence of high salt or low pH (Zhirnov *et al.,* 1992). At high salt (500 mM NaCl) or at low pH (≤pH 5), the isolated viral protein and recombinant M1 behave as normal soluble proteins without the need for detergent (Elster *et al.,* 1997). The low pH or the high salt is probably needed for neutralization of the head groups of the phospholipids or for breaking M1–M1 interactions.

Sha and Luo (1997) determined the atomic structure of the N-terminal two thirds of M1. They proposed that the structure has to fold inside-out for hydrophobic interaction with the membrane and suggested that the hydrophobic residues of helices 1 and 4 would be membrane inserted. However, these residues do not quite correspond with the hydrophobic peptides that Gregoriades (1980) suggested were membrane embedded (i.e., the C-terminus of helix 4, the C-terminus of helix 7, and all of helix 8 but not helix 1). Recently, Shishkov *et al.* (1999) published a tritium bombardment experiment on intact influenza A virus that was supposed to show the parts of M1 protein that are most oriented toward the outside of the virus, whether membrane embedded or not. Their results do not agree with the M1 membrane embedding hypothesis of Sha and Luo (1997) or with the supposed intramembrane peptides proposed by Gregoriades (1980). They found no label on helix 1, and only the N-terminus of helix 4 was labeled. Further, only the N-terminus of helix 7 was labeled, not helix 8. In fact, Shishkov *et al.* (1999) suggest that it is the C-terminal part of M1 that is closest to the outside of the virus and thus closest to the membrane.

If M1 interacts with membranes through electrostatic interactions, then there is no need for inside-out unfolding of M1. Lenard (1996) proposed that the matrix proteins of the negative-strand RNA viruses and the retroviruses are all in one family. Recently, Harris *et al.* (1999) claimed structural similarities between the matrix protein of influenza virus and parts of the matrix and capsid proteins of HIV. The matrix proteins of the retroviruses are not membrane inserted but interact with the negatively charged inside of cell and viral membranes through a polybasic region at the top of the molecule (Matthews *et al.,* 1994; Rao *et al.,* 1995; Hill *et al.,* 1996;

Massiah *et al.,* 1996; Conte *et al.,* 1997; Zhou *et al.,* 1994). Although the secondary structure elements that support this polybasic sequence are not always the same (sometimes β-strands and sometimes α-helices), the basic residues always fall on one side of the molecule (for a review, see Conte and Matthews, 1998). Electrostatic interactions involved in membrane association have also been suggested for $p21^{ras}$ and for a large number of myristoylated proteins (Hancock *et al.,* 1990; Murray *et al.,* 1997).

The N-terminus of influenza M1 also has a polybasic sequence concentrated into a well-delimited patch at one side of the molecule (Sha and Luo, 1997). This patch contains the nuclear localization sequence (NLS) that has recently been shown to be involved in the binding of M1 to naked RNA (Watanabe *et al.,* 1996; Elster *et al.,* 1997). However, in RNP the viral RNA is complexed with NP, which binds to the phosphate-sugar backbone (Baudin *et al.,* 1994), so M1 would have to compete with NP for interaction with the phosphates. This is an unlikely scenario because the affinity of NP for RNA is 10 times stronger than the affinity of M1 for RNA (Baudin *et al.,* 1994; Elster *et al.,* 1997). If the NLS were directed toward the membrane, it could interact with negatively charged head groups of the lipids, and membrane interaction of the influenza virus and retrovirus matrix proteins would perhaps be similar. Unfortunately, in the report of Shishkov (1999), the M1 protein after tritium bombardment was analyzed after trypsin treatment and the authors have not recovered the RKLKR sequence of the NLS, so there is no information on whether the NLS is membrane near or not. Robertson *et al.* (1982) performed dansylation of the influenza virus proteins. The dansyl chromophore is supposed to be membrane restricted, and the authors found specific labeling of lysine residues in M1 that were thought to be located near the viral membrane. One of the peptides that had two labeled lysines included the NLS. Further *in vitro* experiments on the membrane interaction of M1 mutants that miss the NLS sequence will be necessary to positively prove that this sequence is involved in membrane binding. It may be difficult to conduct experiments with recombinant viruses that miss the NLS because a virus with such a mutation will probably not be viable.

MATERIALS AND METHODS

Virus and M1 protein from virus

Influenza virus A/PR/8/34 was grown in embryonated hen's eggs and obtained in purified form from Pasteur-Mérieux-Connaught (Marcy L'Etoile, France). M1 protein was isolated from spikeless virus. Spikes were removed through bromelain digestion (Brand and Skehel, 1972), which was stopped by the addition of 100 mM iodoacetamide. Spikeless virus was then purified by pelleting through 14% sucrose in PBS (150 mM NaCl, 10 mM phosphate buffer, pH 7.2, 0.02% sodium azide). Then the virus was disrupted with 1% Triton X-100 in PBS and spun over a 10–30% continuous glycerol gradient in PBS (SW41 rotor, 36,000 rpm, 4°C, 16 h) and was harvested as shown in Fig. 2.

Recombinant M1 protein

The gene for M1 (A/PR/8/34 strain), as described by Elster *et al.* (1997), was subcloned to remove the sequence coding for the poly-His tail. The new plasmid was expressed in *Escherichia coli* BL21(DE3) pLysS after induction with isopropyl β-D-thiogalactoside at 30°C. The bacteria were opened up through sonication, and M1 was purified through a two-step FPLC protocol using, first, a ion exchange column (SP Sepharose FF) and, second, a gel-exclusion column (Superose 12). During purification, the protein was kept at pH 5.7 in a 10 mM 2-(*N*-morpholino)ethanesulfonic acid-KOH buffer.

Electron microscopy

For negative staining, virus or protein was adsorbed to the clean side of a carbon film on mica (mica/carbon interface), negatively stained with 1% SST, air dried, and observed with the use of a JEOL 1200 EX-II electron microscope under low-dose conditions. Measurements were made from prints with a magnification of 200K using an ocular eyepiece that provided additional magnification of 8×.

Photolabeling of M1 in virus

^{125}I-TID-BE (1 μCi) was dried in an Eppendorf tube, and then 20 μg of A/PR/8/34 was added (PBS, pH 7.3, final volume 20 μl). After 10 min of incubation at room temperature, the sample was photolysed by irradiation for 30 s in a Pyrex vessel mounted approximately 10 cm from an SUSS LH 1000 lamp house (Karl Suss, Waterbury Center, VT) equipped with a 350-W high-pressure mercury lamp. Three volumes of chloroform/methanol (1:2; v/v) were added to the photolabeled virus. After 1 h at room temperature, the precipitated protein was sedimented in an Eppendorf centrifuge (10 min; 14,000 rpm). After removal of the supernatant, the protein pellet was dried under reduced pressure and subjected to 12% SDS–PAGE. The gel was stained with Coomassie Brilliant Blue R-250 and subjected to autoradiography (PhosphorImager).

Recombinant M1 liposome floatation experiments.

Commercial preparations (Sigma Chemical Co.) of phosphatidylcholine (PC), phosphatidylserine (PS), and cholesterol were dissolved in organic solvents (1 mg of lipid total) and dried *in vacuo*. We used two different methods to make M1 liposome complexes essentially as described by Zakowski *et al.* (1981). (1) For the preformed

liposomes, after the addition of 1 ml of 0.2 M Na_2HPO_4/0.1 M citrate, 150 mM NaCl, pH 4, the buffer/lipid mixture was sonicated for 20 min. Then M1 was added (5.5 μM final concentration) to the preformed liposomes and incubated overnight at 4°C. (2) One milliliter of M1 (5.5 μM final concentration) in the same buffer as above plus 34 mM *n*-octyl β-D-glycopyranoside (Sigma) was added to the dried lipids and then mixed on a vortex mixer for 5 min; the detergent was removed through overnight dialysis at 4°C. The lipid compositions of the liposomes are specified in Fig. 4. Then sucrose was added to the two types of M1 liposomes to make them 35% (1.7 ml), and a linear 0–30% gradient of sucrose (3 ml) in the same buffer was formed on top of the 35% sucrose/M1 liposome mixture in sw55 tubes. Gradients were centrifuged for 16 h at 45,000 rpm. A total of six or seven fractions were collected from the top of the gradient plus any remaining pellet that was then taken up in the same fraction volume and were analyzed on 15% SDS–PAGE and stained with Coomassie G250.

M1 cellular membrane sedimentation assays.

Coupled transcription/translation. The M1 gene from influenza virus (A/WSN) was cloned into the pBluescript vector, behind the T7 promoter (pBS-M1). Approximately 1 μg of pBS-M1 was incubated with a TnT Quick Master Mix (Promega, Madison, WI) with 20 μCi of [^{35}S]methionine-cysteine Pro-Mix (Amersham) according to the manufacturer's instructions. To confirm that M1 was soluble, TnT lysates were centrifuged at 125,000 × g for 60 min, and analysis by SDS–PAGE and autoradiography showed that M1 was found in the 125,000 × g supernatant (not shown). As a control protein, we used *in vitro* transcribed/translated GST that was produced through direct translation from a PCR product. Primers corresponding to the T7 promoter/GST N-terminus and the GST C-terminus were synthesized, and a PCR product was generated from the pYEX-4T plasmid (Clontech). Approximately 0.8 μg of the PCR product was incubated with TnT Master Mix as above to generate a soluble GST protein.

Preparation of total cellular membranes. MDCK cells were grown according to standard procedures (Martin and Helenius, 1991). Approximately 2×10^7 MDCK cells were washed on ice with buffer A (0.25 M sucrose, 10 mM triethanolamine, 1 mM EDTA, pH 7.4) and harvested by scraping into a homogenization buffer consisting of 85% (v/v) buffer A plus 15% buffer B (10 mM Tris, pH 7.4, 5 mM KCl, 1 mM EDTA, 128 mM NaCl). Cells were lysed at 4°C with 20 strokes through a 25-gauge needle. A postnuclear supernatant was prepared and centrifuged at 125,000 × g for 60 min at 4°C. The total membrane pellet was resuspended in buffer B, aliquoted, and stored at −80°C.

Membrane binding and release assay. To test for membrane binding, soluble *in vitro* transcribed/translated M1 or control protein was incubated with 1×10^6 cell equivalents of total cellular membranes in 50 mM sodium phosphate buffer, pH 5.5 (or in other buffers as indicated in the legend of Fig. 5) at 37°C for 30 min and then centrifuged at 125,000 × g for 60 min at 4°C in a TLA100.3 rotor. The membrane pellet was lysed in SDS–PAGE sample buffer and analyzed by SDS–PAGE and autoradiography. For the flotation control, the pelleted material was resuspended in 0.8 ml of phosphate buffer containing 80% sucrose, layered on the bottom of a 30–65% discontinuous sucrose gradient, and centrifuged for 18 h at 4°C in a TLS55 rotor at 50,000 rpm. To test for stable association with membranes, a release assay was performed. Membrane-bound M1 was resuspended in 50 mM sodium phosphate buffer, pH 5.5 (or in other buffers as indicated in the legend of Fig. 5), and after 60 min at 37°C, membranes were repelleted at 125,000 × g for 60 min and analyzed by SDS–PAGE and autoradiography.

ACKNOWLEDGMENTS

We thank Dr. Nena Winand (Cornell University) for help with the expression of GST products, Amy Glaser and Elizabeth Wills for experimental help, and Frank Booy, Ruth Collins, Stephen Cusack, Stephen Fuller, and Yves Gaudin for discussions and critical comments on the manuscript. This work was supported by the Schweizerische Nationalfonds and funds from the College of Veterinary Medicine, Cornell University.

REFERENCES

Avalos, R. T., Yu, Z. and Nayak, D. P. (1997). Association of influenza virus NP and M1 proteins with cellular cytoskeletal elements in influenza virus-infected cells. *J. Virol.* **71**, 2947–2958.

Baudin, F., Bach, C., Cusack, S., and Ruigrok, R. W. H. (1994). Structure of influenza virus RNP. I. Influenza virus nucleoprotein melts secondary structure in panhandle RNA and exposes the bases to the solvent. *EMBO J.* **13,** 3158–3165.

Booy, F. P., Ruigrok, R. W. H., and van Bruggen, E. F. J. (1985). Electron microscopy of influenza virus: A comparison of negatively stained and ice-embedded particles. *J. Mol. Biol.* **184,** 667–676.

Brand, C. M., and Skehel, J. J. (1972). Crystalline antigen from the influenza virus envelope. *Nat. New Biol.* **238,** 145–147.

Brunner, J. (1989). Photochemical labeling of the apolar phase of membranes. *Methods Enzymol.* **172,** 628–687.

Brunner, J. (1993). New photolabeling and crosslinking methods. *An. Rev. Biochem.* **62,** 483–514.

Bucher, D. J., Kharitonenkov, I. G., Zakomirdin, J. A., Grigoriev, V. B., Klimenko, S. M., and Davis, J. F. (1980). Incorporation of influenza virus M-protein into liposomes. *J. Virol.* **36,** 586–590.

Conte, M. R., Klikova, M., Hunter, E., Ruml, T., and Matthews, S. (1997). The three-dimensional solution structure of the matrix protein from the type D retrovirus, the Mason-Pfizer monkey virus, and implications for the morphology of retroviral assembly. *EMBO J.* **16,** 5819–5826.

Conte, M. R., and Matthews, S. (1998). Retroviral matrix proteins: A structural perspective. *Virology* **246,** 191–198.

Durrer, P., Gaudin, Y., Ruigrok, R. W. H., Graf, R., and Brunner, J. (1995). Photolabeling identifies a putative fusion domain in the envelope

glycoprotein of rabies and vesicular stomatitis virus. *J. Biol. Chem.* **270,** 17575–17581.

Elster, C., Fourest, E., Baudin, F., Larsen, K., Cusack, S., and Ruigrok, R. W. H. (1994). A small percentage of influenza virus M1 protein contains zinc but zinc does not influence *in vitro* M1 RNA interaction. *J. Gen. Virol.* **75,** 37–42.

Elster, C., Larsen, K., Gagnon, J., Ruigrok, R. W. H., and Baudin, F. (1997). Influenza virus M1 protein binds to RNA through its nuclear localisation signal. *J. Gen. Virol.* **78,** 1589–1596.

Enami, M., and Enami, K. (1996). Influenza virus hemagglutinin and neuraminidase glycoproteins stimulate the membrane association of the matrix protein. *J. Virol.* **70,** 6653–6657.

Fujiyoshi, Y., Kume, N. P., Sakata, K., and Sato, S. B. (1994). Fine structure of influenza A virus observed by electron cryo-microscopy. *EMBO J.* **13,** 318–326.

Gaudin, Y., Ruigrok, R. W. H., and Brunner, J. (1995). Low-pH induced conformational changes in viral fusion proteins: Implications for fusion mechanism. *J. Gen. Virol.* **76,** 1541–1556.

Gregoriades, A. (1980). Interaction of influenza M protein with viral lipid and phosphatidylcholine vesicles. *J. Virol.* **36,** 470–479.

Gregoriades, A., and Frangione, B. (1981). Insertion of influenza M protein into the viral lipid bilayer and localization of site of insertion. *J. Virol.* **40,** 323–328.

Hancock, J. F., Paterson, H., and Marshall, C. J. (1990). A polybasic domain or palmitoylation is required in addition to the CAAX motif to localize $p21^{ras}$ to the plasma membrane. *Cell* **63,** 133–139.

Harris, A., Sha, B., and Luo, M. (1999). Structural similarities between influenza virus matrix protein M1 and human immunodeficiency virus matrix and capsid proteins: An evolutionary link between negative-stranded RNA viruses and retroviruses. *J. Gen. Virol.* **80,** 863–869.

Hill, C. P., Worthylake, D., Bancroft, D. P., Christensen, A. M., and Sundquist, W. I. (1996). Crystal structures of the trimeric human immunodeficiency virus type 1 matrix protein: Implications for membrane association and assembly. *Proc. Natl. Acad. Sci. USA* **93**, 3099–3104.

Jin, H., Leser, G. P., Zhang, J., and Lamb, R. A. (1997). Influenza virus hemagglutinin and neuraminidase cytoplasmic tails control particle shape. *EMBO J.* **16,** 1236–1247.

Kretzschmar, E., Bui, M., and Rose, J. K. (1996). Membrane association of influenza virus matrix protein does not require specific hydrophobic domains or the viral glycoproteins. *Virology* **220,** 37–45.

Lamb, R. A. (1989). Genes and proteins of the influenza viruses. *In* "The Influenza Viruses" (R. M. Krug, Ed.), pp. 1–87, Plenum Press, New York/London.

Lamb, R. A., and Krug, R. M. (1996). Orthomyxoviridae: The viruses and their replication. *In* "Fields' Virology," 3nd ed. (B. N. Fields, D. M. Knipe, P. M. Howley, *et al.*, Eds.) Lippincott-Raven Publishers, Philadelphia.

Lenard, J. (1996). Negative strand virus M and retrovirus MA proteins: All in a family? *Virology* **216**, 289–298.

Martin, K., and Helenius, A. (1991). Transport of incoming influenza virus nucleocapsids into the nucleus. *J. Virol.* **65,** 232–244.

Massiah, M. A., Worthylake, D., Christensen, A. M., Sundquist, W. I., Hill, C. P., and Summers, M. F. (1996). Comparison of the NMR and X-ray structures of the HIV-1 matrix protein: Evidence for conformational changes during viral assembly. *Prot. Sci.* **5**, 2391–2398.

Matthews, S., Barlow, P., Boyd, J., Barton, G., Russell, R., Mills, H., Cunningham, M., Meyers, N., Burns, N., Clark, N., Kingsman, S., Kingsman, A., and Campbell, I. (1994). Structural similarity between the p17 matrix protein of HIV-1 and interferon-γ. *Nature* **370,** 666–668.

Mitnaul, L. J., Castrucci, M. R., Murti, K. G., and Kawaoka, Y. (1996). The cytoplasmic tail of influenza virus neuraminidase (NA) affects incorporation into virions, virion morphology, and virulence in mice but is not essential for virus replication. *J. Virol.* **70,** 873–879.

Murray, D., Ben-Tal, N., Honig, B., and McLaughlin, S. (1997). Electrostatic interaction of myristoylated proteins with membranes: Simple physics, complicated biology. *Structure* **5,** 985–989.

Murti, K. G., Brown, P. S., Bean, W. J., Jr., and Webster, R. G. (1992). Composition of the helical internal component of influenza virus as revealed by immunogold labeling/electron microscopy. *Virology* **186,** 294–299.

Nermut, M. V. (1972). Further investigation on the fine structure of influenza virus. *J. Gen. Virol.* **17,** 317–331.

Oxford, J. S., and Hockley, D. J. (1987). Orthomyxoviridae. *In* "Animal Virus Structure" (M. V. Nermut and A. C. Steven, Eds.), pp. 213–232. Elsevier, Amsterdam.

Rao, Z., Belyaev, A. S., Fry, E., Roy, P., Jones, I. M., and Stuart, D. I. (1995). Crystal structure of SIV matrix antigen and implications for virus assembly. *Nature* **378,** 743–747.

Robertson, B. H., Bennett, J. C., and Compans, R. W. (1982). Selective dansylation of M protein within intact influenza virions. *J. Virol.* **44,** 871–876.

Ruigrok, R. W. H., and Baudin, F. (1995). Structure of influenza virus RNP. II. Purified, RNA-free influenza ribonucleoprotein forms structures that are indistinguishable from the intact viral ribonucleoprotein particles. *J. Gen. Virol.* **76,** 1009–1014.

Ruigrok, R. W. H., Calder, L. J., and Wharton, S. A. (1989). Electron microscopy of the influenza virus submembranal structure. *Virology* **173,** 311–316.

Ruigrok, R. W. H., Wrigley, N. G., Calder, L. J., Cusack, S., Wharton, S. A., Brown, E. B., and Skehel, J. J. (1986). Electron microscopy of the low pH structure of influenza virus haemagglutinin. *EMBO J.* **5,** 41–49.

Schulze, I. T. (1972). The structure of influenza virus. II. A model based on the morphology and composition of subviral particles. *Virology* **47,** 181–196.

Sha, B., and Luo, M. (1997). Structure of a bifunctional membrane-RNA binding protein, influenza virus matrix protein. *Nat. Struct. Biol.* **4,** 239–244.

Shishkov, A. V., Goldanskii, V. I., Baratova, L. A., Fedorova, N. V., Ksenofontov, A. L., Zhirnov, O. P., and Galkin, A. V. (1999). The *in situ* spatial arrangement of the influenza virus matrix protein M1 assessed by tritium bombardment. *Proc. Natl. Acad. Sci. USA* **96,** 7827–7830.

Watanabe, K., Handa, H., Mizumoto, K., and Nagata, K. (1996). Mechanism for inhibition of influenza virus RNA polymerase activity by matrix protein. *J. Virol.* **70,** 241–247.

Wrigley, N. G. (1979). Electron microscopy of influenza virus. *Br. Med. Bull.* **35,** 35–38.

Ye, Z., Pal, R., Fox, J. W., and Wagner, R. R. (1987). Functional and antigenic domains of the matrix (M1) protein of influenza A virus. *J. Virol.* **61,** 239–246.

Zakowski, J. J., Petri, W. A., and Wagner, R. R. (1981). Role of matrix protein in assembling the membrane of vesicular stomatitis virus: Reconstitution of the matrix proteins with negatively charged phospholipid vesicles. *Biochemistry* **20,** 3902–3907.

Zhang, J., and Lamb, R. A. (1996). Characterization of the membrane association of the influenza virus matrix protein in living cells. *Virology* **225,** 255–266.

Zhao, H., Ekström, M., and Garoff, H. (1998). The M1 and NP proteins of influenza A virus form homo- but not heterooligomeric complexes when co-expressed in BHK-21 cells. *J. Gen. Virol.* **79,** 2435–2346.

Zhirnov, O. P. (1992). Isolation of matrix protein from influenza virus by acid-dependent extraction with nonionic detergent. *Virology* **186,** 324–330.

Zhou, W., Parent, L. J., Wills, J. W., and Resh, M. D. (1994). Identification of a membrane-binding domain within the amino-terminal region of human immunodeficiency virus type 1 gag protein which interacts with acidic phospholipids. *J. Virol.* **68,** 2556–2569.